crystals

MDPI

Article

$H_2XP:OH_2$ Complexes: Hydrogen *vs.* Pnicogen Bonds

Ibon Alkorta [1,*], Janet E. Del Bene [2,*] and Jose Elguero [1]

1 Instituto de Química Médica (CSIC), Juan de la Cierva, 3. E-28006 Madrid, Spain; iqmbe17@iqm.csic.es
2 Department of Chemistry, Youngstown State University, Youngstown, OH 44555, USA
* Correspondence: ibon@iqm.csic.es (I.A.); jedelbene@ysu.edu (J.E.D.B.)

Academic Editor: Sławomir Grabowski
Received: 6 January 2016; Accepted: 28 January 2016; Published: 2 February 2016

Abstract: A search of the Cambridge Structural Database (CSD) was carried out for phosphine-water and arsine-water complexes in which water is either the proton donor in hydrogen-bonded complexes, or the electron-pair donor in pnicogen-bonded complexes. The range of experimental P-O distances in the phosphine complexes is consistent with the results of *ab initio* MP2/aug'-cc-pVTZ calculations carried out on complexes $H_2XP:OH_2$, for X = NC, F, Cl, CN, OH, CCH, H, and CH_3. Only hydrogen-bonded complexes are found on the $H_2(CH_3)P:HOH$ and $H_3P:HOH$ potential surfaces, while only pnicogen-bonded complexes exist on $H_2(NC)P:OH_2$, $H_2FP:OH_2$, $H_2(CN)P:OH_2$, and $H_2(OH)P:OH_2$ surfaces. Both hydrogen-bonded and pnicogen-bonded complexes are found on the $H_2ClP:OH_2$ and $H_2(CCH)P:OH_2$ surfaces, with the pnicogen-bonded complexes more stable than the corresponding hydrogen-bonded complexes. The more electronegative substituents prefer to form pnicogen-bonded complexes, while the more electropositive substituents form hydrogen-bonded complexes. The $H_2XP:OH_2$ complexes are characterized in terms of their structures, binding energies, charge-transfer energies, and spin-spin coupling constants $^{2h}J(O\text{-}P)$, $^{1h}J(H\text{-}P)$, and $^{1}J(O\text{-}H)$ across hydrogen bonds, and $^{1p}J(P\text{-}O)$ across pnicogen bonds.

Keywords: hydrogen bonds; pnicogen bonds; CSD; ab initio calculations; structures and binding energies; charge-transfer energies; EOM-CCSD spin-spin coupling constants

1. Introduction

Chloroform, dichloromethane, and water have been observed as solvent molecules in X-ray structures of crystals [1–6]. Such structures have long been used as a tool for identifying and confirming the presence of weak intermolecular interactions. The most prevalent intermolecular interaction in the Cambridge Structural Database (CSD) is the X-H $\cdots$ Y hydrogen bond, which has been at the forefront of intermolecular interactions since Pimentel's book "The Hydrogen Bond" [7]. The hydrogen bond is defined as an attractive interaction between a hydrogen atom from a molecule or a molecular fragment X–H in which X is more electronegative than H, and an atom or a group of atoms in the same or a different molecule, in which there is evidence of bond formation [8,9]. Of particular interest are the hydrogen bonds in the X-ray structures of organic hydrates. Hydrogen bonds involving water molecules interacting with different chemical groups have been identified and classified [3–6].

A relatively new intermolecular interaction, the pnicogen bond, was initially detected in the crystal structures of 1,2-dicarba-*closo*-dodecaboranes [10,11] and aminoalkyl-ferrocenylphosphanes [12]. The structures of two of these complexes are illustrated in Figure 1. A large number of intermolecular and intramolecular pnicogen interactions have also been observed in the solid phase [13–15]. Pnicogen bonds were first described theoretically for model complexes [16,17], and subsequent studies confirmed the stabilizing nature of pnicogen interactions [18–20]. The pnicogen bond is a Lewis acid-Lewis base interaction in which the Lewis acid is a group 15 element (N, P, As, or Sb) acting as an electron-pair acceptor.

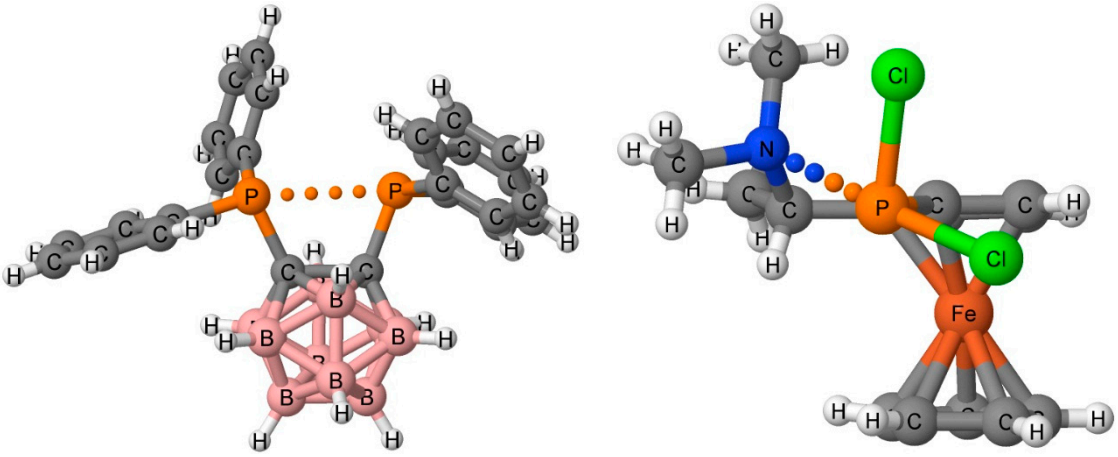

Figure 1. X-ray structure of Cambridge Structural Database (CSD) Refcodes (**a**) XEBBEM01 and (**b**) QEZDOP. The pnicogen bond interaction is indicated with dots.

In the present article, we present the results of our search of the CSD for phosphine-water and arsine-water complexes in which water is either the proton donor in hydrogen-bonded complexes, or the electron-pair donor in pnicogen-bonded complexes. We also report the results of *ab initio* calculations on a series of complexes $H_2XP{:}OH_2$, for X = NC, F, Cl, CN, OH, CCH, H, and CH_3, stabilized by either hydrogen bonds or pnicogen bonds. We present and discuss the structures, binding energies, and charge-transfer energies of these complexes, as well as equation-of-motion coupled cluster singles and doubles (EOM-CCSD) spin–spin coupling constants across hydrogen bonds and pnicogen bonds.

2. Methods

2.1. Cambridge Structural Database Search

The Cambridge Structural Database [21] version 5.36 with updates from November 2014, February 2015, and May 2015 was searched for complexes that contain P(III) and As(III) with water molecules. Included structures have a distance of 2.0 to 4.0 Å between the pnicogen atom and the oxygen atom of water.

2.2. Ab Initio *Calculations*

The structures of the isolated monomers and the binary complexes $H_2XP{:}OH_2$ were optimized at second-order Møller-Plesset perturbation theory (MP2) [22–25] with the aug'-cc-pVTZ basis set [26]. This basis set is derived from the Dunning aug-cc-pVTZ basis set [27,28] by removing diffuse functions from H atoms. Frequencies were computed to establish that the optimized structures correspond to equilibrium structures on their potential surfaces. Optimization and frequency calculations were performed using the Gaussian 09 program [29]. The binding energies (ΔE) of all complexes have been calculated as the total energy of the complex minus the sum of the total energies of the corresponding isolated monomers.

The electron densities of complexes have been analyzed using the Atoms in Molecules (AIM) methodology [30–33] employing the AIMAll [34] program. The topological analysis of the electron density produces the molecular graph of each complex. This graph identifies the location of electron density features of interest, including the electron density (ρ) maxima associated with the various nuclei, and saddle points which correspond to bond critical points (BCPs). The zero gradient line which connects a BCP with two nuclei is the bond path.

The Natural Bond Orbital (NBO) [35] method has been used to analyze the stabilizing charge-transfer interactions using the NBO6 program [36]. Since MP2 orbitals are nonexistent, the charge-transfer interactions have been computed using the B3LYP functional [37,38] with the aug'-cc-pVTZ basis set at the MP2/aug'-cc-pVTZ complex geometries, so that at least some electron correlation effects could be included.

Spin-spin coupling constants were evaluated using the EOM-CCSD method in the CI (configuration interaction)-like approximation [39,40], with all electrons correlated. For these calculations, the Ahlrichs [41] qzp basis set was placed on ^{13}C, ^{15}N, ^{17}O, and ^{19}F, and the qz2p basis set on ^{31}P, ^{35}Cl, and hydrogen-bonded ^{1}H atoms. The Dunning cc-pVDZ basis set was placed on all other ^{1}H atoms. All terms, namely, the paramagnetic spin-orbit (PSO), diamagnetic spin orbit (DSO), Fermi contact (FC), and spin dipole (SD), have been evaluated. The EOM-CCSD calculations were performed using ACES II [42] on the IBM Cluster 1350 (Glenn) at the Ohio Supercomputer Center.

3. Results and Discussion

3.1. CSD Search

The CSD search found only three water-phosphine complexes and seven water-arsine complexes that have a distance of 2.0 to 4.0 Å between the pnicogen atom and the oxygen atom of water. Two of the water–phosphine complexes are hydrogen bonded (CSD Refcodes: AGAHIB and BEZTOR) with P···H distances of 2.48 and 2.72 Å, and P···O distances of 3.315 and 3.465 Å, respectively. The third structure (NOPYEX) corresponds to a pnicogen-bonded complex between a triphenylphosphine derivative and water with a longer P···O distance of 3.76 Å. Four of the water-arsine complexes (TELFAR, NOPYAT, FUTDUU, and IBAKIH) are pnicogen-bonded, and three (NIVWAQ, FUTDUU, and HAVKEW) are hydrogen-bonded. The pnicogen-bonded complex TELFAR which is illustrated in Figure 2 has a short As-O pnicogen bond distance of 2.56 Å. The O-As-O angle is 171°, which allows for the interaction of the O of water with the σ-hole of As. The short distance for this bond suggests that it has significant covalent character. The As···O distances in the other pnicogen-bonded complexes range between 3.61 and 3.78 Å. The hydrogen-bonded complexes have As···H distances between 2.81 and 3.22 Å, and As···O distances between 3.70 and 3.96 Å.

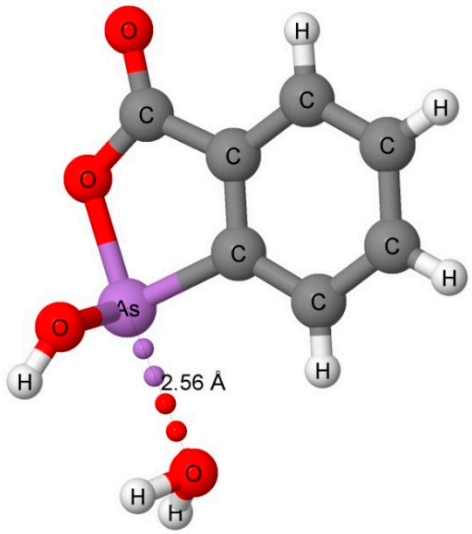

Figure 2. The X-ray structure of CSD Refcode: TELFAR showing the As···O pnicogen bond interaction.

3.2. Computational Results

We have attempted to optimize eight complexes H_2XP:HOH with O-H··· P hydrogen bonds, and eight complexes with P··· O pnicogen bonds, with X = NC, F, Cl, CN, OH, CCH, H, and CH_3.

However, only four hydrogen-bonded (HB) and six pnicogen-bonded (ZB) equilibrium complexes have been found on the potential surfaces. The structures, total energies, and molecular graphs of these complexes are reported in Table S1 of the Supporting Information, and their binding energies are given in Table 1. ZB complexes have binding energies which vary from –11.3 to –21.1 kJ· mol^{-1}, while HB complexes have binding energies between –9.4 and –15.4 kJ· mol^{-1}. The absolute values of the binding energies of the ZB complexes decrease in the order

$$NC > F > Cl > CN > OH > CCH$$

while those of the HB complexes decrease in the reverse order

$$CH_3 > H > CCH > Cl.$$

It is apparent from Table 1 that the more electronegative substituents prefer to form pnicogen-bonded complexes, while the more electropositive substituents form hydrogen-bonded complexes. This trend follows the general trend of the Molecular Electrostatic Potential (MEP) values around the phosphorous atom [43]. H_2ClP and H(CCH)P form both hydrogen-bonded and pnicogen-bonded complexes with H_2O, with the latter more stable by 7.9 and 0.5 kJ·mol^{-1}, respectively.

Table 1. Binding energies of equilibrium pnicogen-bonded (ZB) and hydrogen-bonded (HB) complexes of H_2XP with H_2O.

H_2XP, X =	Binding Energies (ΔE, kJ· mol^{-1})	
	ZB	**HB**
NC	–21.1	
F	–19.5	
Cl	–17.3	–9.4
CN	–16.9	
OH	–12.8	
CCH	–11.3	–10.8
H		–11.1
CH_3		–15.4

3.2.1. Hydrogen-Bonded Complexes

Only four equilibrium hydrogen-bonded complexes have been found on the H_2XP:HOH surfaces; namely, H_2ClP:HOH, H_2(CCH)P:HOH, H_3P:HOH, and $H_2(CH_3)P$:HOH. The binding energies of these are given in Table 1, and selected structural parameters are reported in Table 2. The shortest intermolecular O···P and H···P distances are 3.360 and 2.536 Å, respectively, in $H_2(CH_3)P$:HOH. The remaining three complexes have O···P distances between 3.55 and 3.59 Å, and H···P distances between 2.62 and 2.66 Å. These distances are consistent with the experimental distances from the CSD. As evident from Table 2, the hydrogen bonds in H_2(CCH)P:HOH and H_3P:HOH are close to linear, with H-O-P angles of 7°, while these bonds in H_2ClP:HOH and $H_2(CH_3)P$:HOH are nonlinear with values of 19 and 27°, respectively. Moreover, the H_2O molecule is positioned similarly in H_2ClP:HOH and H_2(CCH)P:HOH, but has a different orientation in H_3P:HOH and $H_2(CH_3)P$:HOH, as illustrated in Figure 3. In these two complexes, but particularly $H_2(CH_3)P$:HOH, there appears to be an attractive interaction between the water oxygen and the hydrogens of the substituent. All of these differences lead to a lack of correlation between the binding energies of these complexes and the O···P distances. However, the electrostatic minimum associated with the lone pair of the phosphorous atom [43] and the H···P distances do correlate. Although not included in Tables 1 and 2 there is an equilibrium hydrogen-bonded complex formed between H_2(OH)P and H_2O with a binding energy of –28.5 kJ·mol^{-1}. However, it is stabilized by an O-H··· O hydrogen bond with the substituent O-H as the proton donor to H_2O.

Table 2. O···P, H···P, and O-H distances, and H-O-P angles for hydrogen-bonded complexes H_2XP:HOH with C_s symmetry.

H_2XP, X =	Distance (R, Å)			Angles (<, °)
	R(O···P)	R(H···P)	R(O-H) [a]	<H-O-P
Cl	3.553	2.656	0.965	19
CCH	3.585	2.629	0.966	7
H	3.575	2.620	0.966	7
CH_3	3.360	2.536	0.967	27

(a) The O-H distance in isolated H_2O is 0.961 Å.

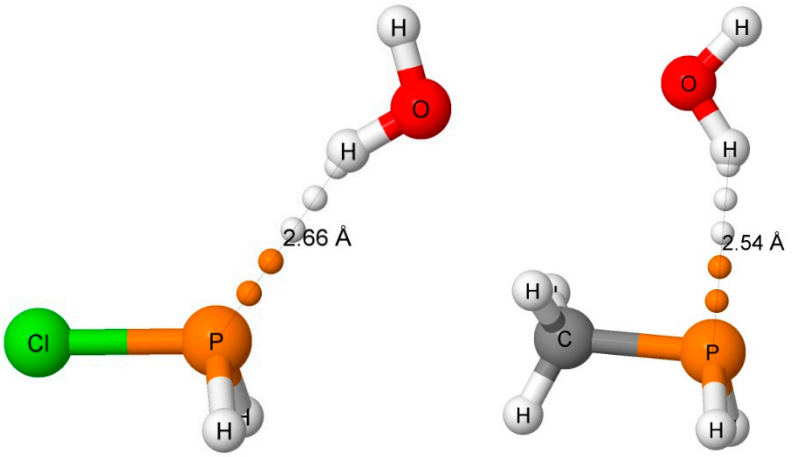

(**a**) (**b**)

Figure 3. The hydrogen-bonded complexes H_2ClP:HOH (**a**) and $H_2(CH_3)P$:HOH (**b**). The orientation of the H_2O molecule in $H_2(CCH)P$:HOH is similar to that in H_2ClP:HOH, while the orientation of H_2O in H_3P:HOH is similar to that in $H_2(CH_3)P$:HOH.

Table 3 presents the stabilizing NBO $P_{lp}\rightarrow\sigma^*$H-O charge-transfer energies for the four hydrogen-bonded complexes. These energies range from 9 kJ·mol^{-1} for H_2ClP:HOH to between 14 and 15 kJ·mol^{-1} for the remaining complexes. The charge-transfer energies do not correlate with either the O···P or the H···P distances.

Table 3. Charge-transfer energies ($P_{lp}\rightarrow\sigma^*$H-O) and coupling constants ^{2h}J(O-P), ^{1h}J(H-P), and ^{1}J(O-H) for hydrogen-bonded complexes H_2XP:HOH.

H_2XP, X =	Charge-Transfer Energies (kJ·mol^{-1})	Coupling Constants (Hz)		
	$P_{lp}\rightarrow\sigma^*$H-O [a]	^{2h}J(O-P)	^{1h}J(H-P)	^{1}J(O-H) [b]
Cl	9.0	–18.2	–12.9	–78.0
CCH	13.8	–14.4	–13.0	–77.9
H	14.0	–14.0	–13.5	–78.1
CH_3	15.0	–24.1	–15.0	–78.4

[a] The $O_{lp}\rightarrow\sigma^*$H-O charge-transfer energy in the complex of $H_2(OH)P$ with H_2O that has the substituent O-H as the proton donor is 41.0 kJ·mol^{-1}; [b] ^{1}J(O-H) in isolated H_2O is –77.0 Hz.

The two-bond coupling constant ^{2h}J(O-P) and the one-bond coupling constant ^{1h}J(H-P) across the hydrogen bonds, and the one-bond coupling constant ^{1}J(O-H) for the hydrogen-bonded O-H group are also reported in Table 3. The components of these coupling constants are reported in Table S2

of the Supporting Information. Values of ^{2h}J(O-P) vary from –14 to –24 Hz, while values of ^{1h}J(H-P) lie between –13 and –15 Hz. The dependence of these two coupling constants on the corresponding O···P and H···P distances is shown graphically in Figure 4. Since there are only 4 points in each set and at least two of them have similar values of the coupling constant and the corresponding distance, only linear trendlines were used to illustrate the distance dependence. The correlation coefficients of these trendlines are 0.915 for ^{2h}J(O-P) and 0.973 for ^{1h}J(H-P). The third coupling constant, ^{1}J(O-H) has a value of –77.0 Hz in the isolated H_2O molecule, and increases in absolute value only slightly upon complex formation to between –77.9 and –78.4 Hz. The O-H distance of 0.961 Å in the monomer also increases only slightly upon complexation, with values between 0.965 and 0.967 Å. The one-bond coupling constant ^{1}J(O-H) for the non-hydrogen-bonded O-H decreases to about –62 Hz.

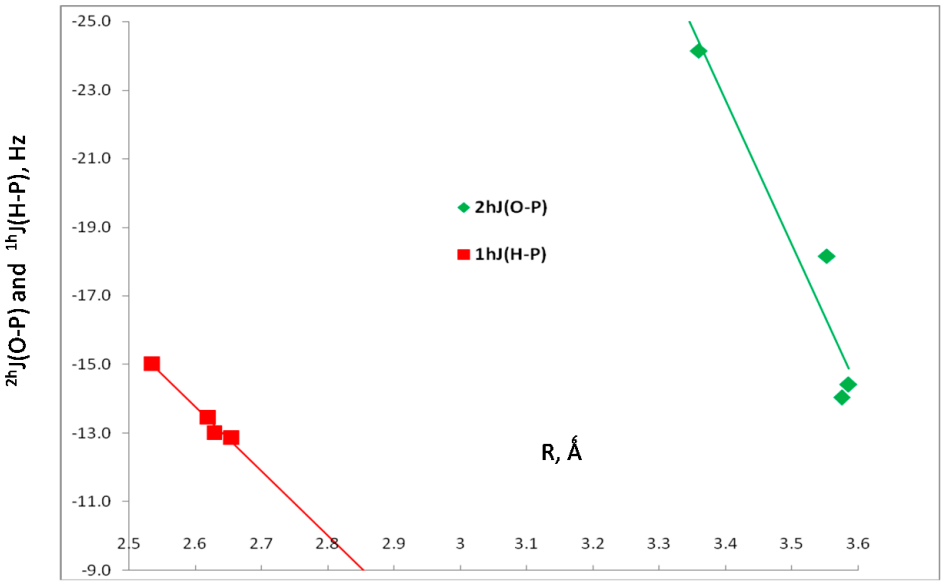

Figure 4. ^{2h}J(O-P) *versus* the O···P distance, and ^{1h}J(H-P) *versus* the H···P distance for HB complexes H_2XP:HOH.

3.2.2. Pnicogen-Bonded Complexes

Three of the six equilibrium pnicogen-bonded H_2XP:OH_2 complexes have C_s symmetry with the H_2O molecule in the symmetry plane, and three have C_1 symmetry. For reasons of computational efficiency, particularly for the coupling constant calculations, we have re-optimized the C_1 structures under the constraint of C_s symmetry with an in-plane H_2O molecule. The binding energies of C_1 and C_s structures are compared in Table 4. The C_s structures of H_2FP:OH_2, H_2ClP:OH_2, and $H_2(OH)P$:OH_2 with H_2O in the C_s symmetry plane are only 0.1 to 0.4 kJ·mol^{-1} less stable than the C_1 equilibrium structures. Moreover, the ordering of complexes according to decreasing binding energy is the same for the equilibrium structures and those with C_s symmetry, and the structures of C_1 and corresponding C_s complexes are very similar. To ensure that there are no other pnicogen-bonded complexes with P···O pnicogen bonds, we also optimized a set of these complexes with C_s symmetry in which the H_2O molecule does not lie in the symmetry plane. All of these complexes have one imaginary frequency, and smaller absolute values of the binding energies than the complexes with in-plane H_2O molecules, as evident from Table 4. The two types of C_s complexes are illustrated in Figure 5.

The structures, total energies, and molecular graphs of the three pnicogen-bonded ZB complexes H_2XP:OH_2 with C_s symmetry, one imaginary frequency, and in-plane H_2O molecules are reported in Table S3 of the Supporting Information. This table also provides these data for the six less-stable ZB complexes with C_s symmetry, one imaginary frequency, and out-of-plane H_2O molecules. Table 5 presents selected data for the more stable C_s complexes with in-plane H_2O molecules. The P···O

distances in these complexes range from 2.755 Å in $H_2FP{:}OH_2$ to 3.036 Å in $H_2(CCH)P{:}OH_2$. Their binding energies do not correlate well with the P···O distances, as indicated by correlation coefficients of 0.7 for linear, quadratic, and exponential trendlines. The O-P-A angles, with A the atom of X directly bonded to P, are also reported in Table 5. These angles vary between 161 and 168°, indicating that the O-P-A arrangement approaches linearity. These values are consistent with the values of the P-P-A and N-P-A angles in the pnicogen-bonded complexes $(H_2XP)_2$ [44] and $H_2XP{:}NXH_2$ [45].

Table 4. Binding energies of pnicogen-bonded complexes with C_1 and C_s symmetries.

H_2XP, X =	Equilibrium Symmetry	ΔE (kJ·mol^{-1}) for Equilibrium Structures	ΔE (kJ·mol^{-1}) for C_s Structures with H_2O in-Plane	ΔE (kJ·mol^{-1}) for C_s Structures with H_2O out-of-Plane
NC	C_s	–21.1	–21.1	–19.9[b]
F	C_1	–19.5	–19.2[a]	–18.5[b]
Cl	C_1	–17.3	–17.2[a]	–16.3[b]
CN	C_s	–16.9	–16.9	–15.7[b]
OH	C_1	–12.8	–12.4[a]	–12.1[b]
CCH	C_s	–11.3	–11.3	–10.1[b]

[a] These C_s structures with water in-plane have one imaginary frequency; [b] These complexes with out-of-plane H_2O molecules have one imaginary frequency.

(**a**) (**b**)

Figure 5. The pnicogen-bonded complexes $H_2ClP{:}OH_2$ (**a**) with the H_2O molecule in the C_s symmetry plane; and $H_2FP{:}OH_2$ (**b**) with C_s symmetry and an out-of-plane H_2O molecule.

Table 5 also presents the NBO $O_{lp}\rightarrow\sigma^*$P-A charge-transfer energies in these pnicogen-bonded complexes. Charge-transfer energies vary from 8 kJ·mol^{-1} in $H_2(CCH)P{:}OH_2$ to 20 kJ·mol^{-1} in $H_2(NC)P{:}OH_2$. They exhibit an exponential dependence on the P···O distance, with a correlation coefficient of 0.949.

Table 5. P···O distances, O-P-A angles, charge-transfer energies, and ^{1p}J(P-O) coupling constants for pnicogen-bonded complexes $H_2XP{:}OH_2$ with C_s symmetry and in-plane H_2O molecules.

H_2XP, X =	Distance (R, Å)	Angles (<, °)	Charge-Transfer Energies (kJ·mol^{-1})	Coupling Constants (Hz)
	R(P···O)	<O-P-A[a]	$O_{lp}\rightarrow\sigma^*$P-A	^{1p}J(P-O)
NC[b]	2.800	165	20.3	–62.5
F	2.755	167	19.5	–69.8
Cl	2.835	166	17.4	–61.2
CN[b]	2.944	161	12.3	–41.9
OH	2.919	166	11.6	–46.7
CCH	3.036	167	8.0	–36.7

[a] A is the atom of X directly bonded to P. [b] The atom written first is directly bonded to P.

Table 5 also reports the spin–spin coupling constants ^{1p}J(P-O) across the pnicogen bonds. The components of these coupling constants are reported in Table S4 of the Supporting Information. ^{1p}J(P-O) values are dominated by the Fermi-contact terms, and vary from –37 Hz in $H_2(CCH)P{:}OH_2$

to –70 Hz in $H_2FP{:}OH_2$. Figure 6 illustrates the second-order dependence of ^{1p}J(P-O) on the P···O distance, with a correlation coefficient of 0.979.

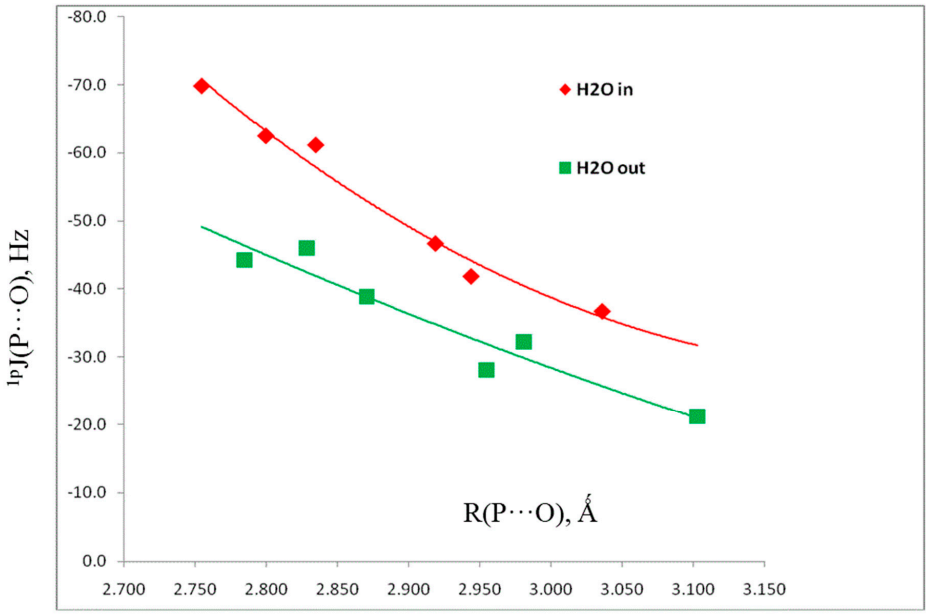

Figure 6. ^{1p}J(P-O) *versus* the P···O distance for pnicogen-bonded complexes $H_2XP{:}OH_2$ with C_s symmetry and in-plane and out-of-plane H_2O molecules.

A second reason for optimizing the set of complexes with C_s symmetry and out-of-plane H_2O molecules is to examine the coupling constants of these structures, the components of which are reported in Table S5. Since ^{1p}J(P-O) values are also dominated by the Fermi-contact terms, it is expected that the s electron densities at O and at P interacting with O will be very different in the ground state and the excited states which couple to the ground state for these two orientations of H_2O molecules. It is apparent from Figure 6 that such is the case, since at the same P···O distances, the points for structures with out-of-plane H_2O molecules lie below those for in-plane H_2O molecules.

Finally, a plot of ^{2h}J(O-P) for hydrogen-bonded complexes and ^{1p}J(P-O) for pnicogen-bonded complexes with C_s symmetry and in-plane H_2O molecules *versus* the P···O distance is reported as Figure S1 of the Supporting Information. At the shorter P···O distances, the absolute values of ^{2h}J(O-P) are greater than the values of ^{1p}J(P-O) at longer distances, but a single second-order trendline with a correlation coefficient of 0.981 describes the distance dependence of both coupling constants.

4. Conclusions

Crystal structures have long been used as a tool for identifying and confirming the presence of weak intermolecular interactions, including hydrogen bonds and pnicogen bonds. A search of the CSD for complexes of water with phosphine and arsine identified two water–phosphine complexes stabilized by hydrogen bonds and one stabilized by a pnicogen bond, as well as three water–arsine complexes with hydrogen bonds and four with pnicogen bonds. The range of P···O distances in the phosphine complexes is consistent with the results of *ab initio* MP2/aug'-cc-pVTZ calculations carried out on complexes $H_2XP{:}OH_2$, for X = NC, F, Cl, CN, OH, CCH, H, and CH_3. Only hydrogen-bonded complexes are found on the $H_2(CH_3)P{:}OH_2$ and $H_3P{:}OH_2$ potential surfaces, while only pnicogen-bonded complexes exist on the $H_2(NC)P{:}OH_2$, $H_2FP{:}OH_2$, $H_2(CN)P{:}OH_2$, and $H_2(OH)P{:}OH_2$ surfaces. Both hydrogen-bonded and pnicogen-bonded complexes are found on the $H_2ClP{:}OH_2$ and $H_2(CCH)P{:}OH_2$ surfaces, with the pnicogen-bonded complexes more stable than the corresponding hydrogen-bonded complexes. It is apparent that the more electronegative

substituents prefer to form pnicogen-bonded complexes, while the more electropositive substituents form hydrogen-bonded complexes. The binding energies of pnicogen-bonded complexes range from –11 to –21 kJ· mol^{-1}, while the pnicogen-bonded complexes have binding energies from –9 to –15 kJ· mol^{-1}. The hydrogen-bonded complexes are stabilized by charge transfer from the lone pair on P to the antibonding σ* H-O orbital, while pnicogen-bonded complexes are stabilized by charge transfer from the lone pair on O to the antibonding σ* P-A orbital, with A the atom of X directly bonded to P.

Spin-spin coupling constants ^{2h}(O-P) and ^{1h}J(H-P) correlate with the O$\cdots$P and H$\cdots$P distances, respectively, while ^{1}J(O-H) for the hydrogen-bonded O-H group increases in absolute value only slightly upon complex formation. ^{1p}J(P-O) coupling constants were computed for two sets of pnicogen-bonded complexes, one with C_s symmetry and the H_2O molecule in the symmetry plane, and the other also with C_s symmetry but with an out-of-plane H_2O molecule. ^{1p}J(P-O) for both sets are quadratically dependent on the P$\cdots$O distance. The different orientations of the H_2O molecule in these two sets alter the s electron densities at O and P, and lead to greater absolute values of ^{1p}J(P-O) for complexes with in-plane H_2O molecules compared to those with out-of-plane H_2O molecules.

Supplementary Materials: Supplementary materials can be found at http://www.mdpi.com/2073-4352/6/2/19/s1.

Acknowledgments: This work was carried out with financial support from the Ministerio de Economía y Competitividad (Project No. CTQ2012-35513-C02-02) and Comunidad Autónoma de Madrid (Project FOTOCARBON, ref. S2013/MIT-2841). Thanks are also given to the Ohio Supercomputer Center and CTI (CSIC) for their continued computational support.

Author Contributions: Ibon Alkorta and Janet E. Del Bene carried out the calculations and analyzed the data. All three authors contributed to the manuscript.

Conflicts of Interest: The authors declare no conflict of interest.

References

1. Allen, F.H.; Wood, P.A.; Galek, P.T.A. Role of chloroform and dichloromethane solvent molecules in crystal packing: An interaction propensity study. *Acta Cryst.* **2013**, *B69*, 379–388. [CrossRef] [PubMed]
2. Van de Streek, J. All series of multiple solvates (including hydrates) from the Cambridge Structural Database. *CrystEngComm* **2007**, *9*, 350–352. [CrossRef]
3. Infantes, L.; Chisholm, J.; Motherwell, S. Extended motifs from water and chemical functional groups in organic molecular crystals. *CrystEngComm* **2003**, *5*, 480–486. [CrossRef]
4. Infantes, L.; Motherwell, S. Water clusters in organic molecular crystals. *CrystEngComm* **2002**, *4*, 454–461. [CrossRef]
5. Gillon, A.L.; Feeder, N.; Davey, R.J.; Storey, R. Hydration in Molecular Crystals-A Cambridge Structural Database Analysis. *Cryst. Growth Des.* **2003**, *3*, 663–673. [CrossRef]
6. Infantes, L.; Fabian, L.; Motherwell, S. Organic crystal hydrates: What are the important factors for formation. *CrystEngComm* **2007**, *9*, 65–71. [CrossRef]
7. Pimentel, G.C.; McClellan, A.L. *The Hydrogen Bond*; W.H. Freeman: San Francisco, CA, USA, 1960.
8. Arunan, E.; Desiraju Gautam, R.; Klein Roger, A.; Sadlej, J.; Scheiner, S.; Alkorta, I.; Clary David, C.; Crabtree Robert, H.; Dannenberg Joseph, J.; Hobza, P.; *et al*. Defining the hydrogen bond: An account (IUPAC Technical Report). *Pure Appl. Chem.* **2011**, *83*, 1619–1636. [CrossRef]
9. Arunan, E.; Desiraju Gautam, R.; Klein, R.-A.; Sadlej, J.; Scheiner, S.; Alkorta, I.; Clary, D.C.; Crabtree, R.H.; Dannenberg, J.J.; Hobza, P.; *et al*. Definition of the hydrogen bond (IUPAC Recommendations 2011). *Pure Appl. Chem.* **2011**, *83*, 1637–1641. [CrossRef]
10. Sundberg, M.R.; Uggla, R.; Viñas, C.; Teixidor, F.; Paavola, S.; Kivekäs, R. Nature of intramolecular interactions in hypercoordinate C-substituted 1,2-dicarba-closo-dodecaboranes with short P$\cdots$P distances. *Inorg. Chem. Commun.* **2007**, *10*, 713–716. [CrossRef]
11. Bauer, S.; Tschirschwitz, S.; Lönnecke, P.; Frank, R.; Kirchner, B.; Clarke, M.L.; Hey-Hawkins, E. Enantiomerically pure bis(phosphanyl)carbaborane(12) compounds. *Eur. J. Inorg. Chem.* **2009**, *2009*, 2776–2788. [CrossRef]

12. Tschirschwitz, S.; Lonnecke, P.; Hey-Hawkins, E. Aminoalkylferrocenyldichlorophosphanes: Facile synthesis of versatile chiral starting materials. *Dalton Trans.* **2007**, 1377–1382. [CrossRef] [PubMed]
13. Politzer, P.; Murray, J.; Janjić, G.; Zarić, S. σ-Hole interactions of covalently-bonded nitrogen, phosphorus and arsenic: A survey of crystal structures. *Crystals* **2014**, *4*, 12–31. [CrossRef]
14. Sánchez-Sanz, G.; Alkorta, I.; Trujillo, C.; Elguero, J. Intramolecular pnicogen interactions in PHF-$(CH_2)_n$-PHF (n = 2–6) systems. *ChemPhysChem* **2013**, *14*, 1656–1665. [CrossRef] [PubMed]
15. Sánchez-Sanz, G.; Trujillo, C.; Alkorta, I.; Elguero, J. Intramolecular pnicogen interactions in phosphorus and arsenic analogues of proton sponges. *Phys. Chem. Chem. Phys.* **2014**, *16*, 15900–15909. [CrossRef] [PubMed]
16. Scheiner, S. A new noncovalent force: Comparison of P···N interaction with hydrogen and halogen bonds. *J. Chem. Phys.* **2011**, *134*, 094315. [CrossRef] [PubMed]
17. Zahn, S.; Frank, R.; Hey-Hawkins, E.; Kirchner, B. Pnicogen bonds: A new molecular linker? *Chem. Eur. J.* **2011**, *17*, 6034–6038. [CrossRef] [PubMed]
18. Scheiner, S. The pnicogen bond: Its relation to hydrogen, halogen, and other noncovalent bonds. *Acc. Chem. Res.* **2012**, *46*, 280–288. [CrossRef] [PubMed]
19. Scheiner, S. Detailed comparison of the pnicogen bond with chalcogen, halogen, and hydrogen bonds. *Int. J. Quantum Chem.* **2013**, *113*, 1609–1620. [CrossRef]
20. Del Bene, J.E.; Alkorta, I.; Elguero, J. The pnicogen bond in review: Structures, binding energies, bonding properties, and spin-spin coupling constants of complexes stabilized by pnicogen bonds. In *Noncovalent Forces*; Challenges and Advances in Computational Chemistry and Physics Series; Scheiner, S., Ed.; Springer: Gewerbestrasse, Switzerland, 2015; Volume 19, pp. 191–263.
21. Allen, F. The Cambridge Structural Database: A quarter of a million crystal structures and rising. *Acta Crystallogr. Sect. B* **2002**, *58*, 380–388. [CrossRef]
22. Pople, J.A.; Binkley, J.S.; Seeger, R. Theoretical models incorporating electron correlation. *Int. J. Quantum Chem. Quantum Chem. Symp.* **1976**, *10*, 1–19. [CrossRef]
23. Krishnan, R.; Pople, J.A. Approximate fourth-order perturbation theory of the electron correlation energy. *Int. J. Quantum Chem.* **1978**, *14*, 91–100. [CrossRef]
24. Bartlett, R.J.; Silver, D.M. Many-body perturbation theory applied to electron pair correlation energies. I. Closed-shell first-row diatomic hydrides. *J. Chem. Phys.* **1975**, *62*, 3258–3268. [CrossRef]
25. Bartlett, R.J.; Purvis, G.D. Many-body perturbation theory, coupled-pair many-electron theory, and the importance of quadruple excitations for the correlation problem. *Int. J. Quantum Chem.* **1978**, *14*, 561–581. [CrossRef]
26. Del Bene, J.E. Proton affinities of ammonia, water, and hydrogen fluoride and their anions: A quest for the basis-set limit using the dunning augmented correlation-consistent basis sets. *J. Phys. Chem.* **1993**, *97*, 107–110. [CrossRef]
27. Dunning, T.H. Gaussian Basis Sets for Use in Correlated Molecular Calculations. I. The Atoms Boron through Neon and Hydrogen. *J. Chem. Phys.* **1989**, *90*, 1007–1023. [CrossRef]
28. Woon, D.E.; Dunning, T.H. Gaussian Basis Sets for Use in Correlated Molecular Calculations. V. Core-Valence Basis Sets for Boron Through Neon. *J. Chem. Phys.* **1995**, *103*, 4572–4585. [CrossRef]
29. Frisch, M.J.; Trucks, G.W.; Schlegel, H.B.; Scuseria, G.E.; Robb, M.A.; Cheeseman, J.R.; Scalmani, G.; Barone, V.; Mennucci, B.; Petersson, G.A.; *et al*. *Gaussian–09, Revision D.01*; Gaussian, Inc.: Wallingford, CT, USA, 2009.
30. Bader, R.F.W. A quantum theory of molecular structure and its applications. *Chem. Rev.* **1991**, *91*, 893–928. [CrossRef]
31. Bader, R.F.W. *Atoms in Molecules, A Quantum Theory*; Oxford University Press: Oxford, UK, 1990.
32. Popelier, P.L.A. *Atoms in Molecules. An Introduction*; Prentice Hall: Harlow, UK, 2000.
33. Matta, C.F.; Boyd, R.J. *The Quantum Theory of Atoms in Molecules: From Solid State to DNA and Drug Design*; Wiley-VCH: Weinheim, Germany, 2007.
34. Keith, T.A. *AIMALL*; Version 15.09.27. TK Gristmill Software: Overland Park, KS, USA, 2011. Available online: http://aim.tkgristmill.com (accessed on 31 December 2015).
35. Reed, A.E.; Curtiss, L.A.; Weinhold, F. Intermolecular interactions from a Natural Bond Orbital, donor-acceptor viewpoint. *Chem. Rev.* **1988**, *88*, 899–926. [CrossRef]
36. Glendening, E.D.; Badenhoop, J.K.; Reed, A.E.; Carpenter, J.E.; Bohmann, J.A.; Morales, C.M.; Landis, C.R.; Weinhold, F. *NBO 6.0*; University of Wisconsin: Madison, WI, USA, 2013.

37. Becke, A.D. Density functional thermochemistry. III. The role of exact exchange. *J. Chem. Phys.* **1993**, *98*, 5648–5652. [CrossRef]
38. Lee, C.; Yang, W.; Parr, R.G. Development of the Colle-Salvetti correlation-energy formula into a functional of the electron density. *Phys. Rev. B* **1988**, *37*, 785789. [CrossRef]
39. Perera, S.A.; Nooijen, M.; Bartlett, R.J. Electron correlation effects on the theoretical calculation of Nuclear Magnetic Resonance spin–spin coupling constants. *J. Chem. Phys.* **1996**, *104*, 3290–3305. [CrossRef]
40. Perera, S.A.; Sekino, H.; Bartlett, R.J. Coupled–cluster calculations of indirect nuclear coupling constants: The importance of non–Fermi-contact contributions. *J. Chem. Phys.* **1994**, *101*, 2186–2196. [CrossRef]
41. Schäfer, A.; Horn, H.; Ahlrichs, R. Fully optimized contracted Gaussian basis sets for atoms Li to Kr. *J. Chem. Phys.* **1992**, *97*, 2571–2577. [CrossRef]
42. Stanton, J.F.; Gauss, J.; Watts, J.D.; Nooijen, M.; Oliphant, N.; Perera, S.A.; Szalay, P.S.; Lauderdale, W.J.; Gwaltney, S.R.; Beck, S.; *et al*. *ACES II*; University of Florida: Gainesville, FL, USA, 2014.
43. Del Bene, J.E.; Alkorta, I.; Elguero, J. Characterizing Complexes with Pnicogen Bonds Involving sp2 Hybridized Phosphorus Atoms: $(H_2C{=}PX)_2$ with X = F, Cl, OH, CN, NC,CCH, H, CH_3, and BH_2. *J. Phys. Chem. A* **2013**, *117*, 6893–6903.
44. Del Bene, J.E.; Alkorta, I.; Sanchez-Sanz, G.; Elguero, J. ^{31}P-^{31}P Spin-spin coupling constants for Pnicogen Homodimers. *Chem. Phys. Lett.* **2011**, *512*, 184–187. [CrossRef]
45. Del Bene, J.E.; Alkorta, I.; Sanchez-Sanz, G.; Elguero, J. Structures, Energies, Bonding, and NMR Properties of Pnicogen Complexes $H_2XP{:}NXH_2$ (X = H, CH_3, NH_2, OH, F, Cl). *J. Phys. Chem. A* **2011**, *115*, 13724–13731. [CrossRef] [PubMed]